ELSEVIER

Journal of Structural Geology 27 (2005) 161–170

JOURNAL OF STRUCTURAL GEOLOGY

www.elsevier.com/locate/jsg

Bedding tilt test for paleostress analysis

Atsushi Yamaji*, Satoshi Tomita, Makoto Otsubo

Division of Earth and Planetary Sciences, Kyoto University, Sakyo-ku, Kyoto 606-8502, Japan

Received 21 February 2003; received in revised form 13 March 2004; accepted 6 August 2004
Available online 1 October 2004

Abstract

It is difficult to apply stress inversion to fault-slip data obtained from highly tilted sedimentary layers, especially in areas where criteria for fault sorting are not available at outcrops. This paper shows that a bedding tilt test similar to that used in paleomagnetism allows paleostresses to be inferred. In order to assess its validity, the testing method was applied firstly to artificial fault-slip data generated with a hypothetical history for folding and faulting with known paleostresses. The stresses were successfully recovered and the correct timing of faulting relative to tilting could be determined. The test procedure was secondly applied to mesoscale faults observed in a mid-Pleistocene sedimentary unit in central Japan, which was folded in late Pleistocene. It was found that the majority of the faults were activated mainly by a strike-slip faulting regime of stress at the middle stage of folding.
© 2004 Elsevier Ltd. All rights reserved.

Keywords: Tectonics; Stress; Fault; Fold; Multiple inverse method; Tilting; Pleistocene; Japan

1. Introduction

Paleostress inversion has some weak points (Pollard et al., 1993; Twiss and Unruh, 1998). Among them is a common problem in structural geology, which is controversial for dating geologic structures. For this reason, tilting of faulted rock masses gives rise to a difficult problem for determining paleostresses (Angelier et al., 1985; Angelier, 1994). If faulting is older than tilting, it is necessary to tilt back the whole system (faults, stress tensor and bedding) in order to restore it into its initial position. If, however, faulting is younger than tilting, no tilt correction is necessary. If the fault activity was simultaneous with progressive tilting, we need to know to what amount the rock mass was rotated when the individual faults were activated.

To cope with this problem, mesoscale faults are usually classified at outcrops by their apparent relative ages (Angelier et al., 1986; Choi et al., 2001; Vandycke and Bergerat, 2001). The principal guides for distinguishing the different fault sets are (1) consideration of stratigraphy or of the age of the rocks affected by a certain deformation, (2) characterization of the syn-sedimentary faults such as fault drag, (3) cross-cutting relationships, (4) superimposed striae on the same fault plane, and (5) association of mineral veins. Unfortunately, these criteria are not always available in the field. The classification is difficult, especially in very young or active belts, because most mesoscale faults look alike, their number density is too low and age of rocks covers a short range.

Problems also come from the fact that the concept of stress fails for deformations with finite rotations. Paleostress inversion determines a Cauchy stress, which is meaningful only for very small incremental deformations. The definition of stress to describe forces in the rock mass that have undergone a finite rotation is not unique (Fung, 1965). However, Cauchy stress is appropriate to describe a force system in the rock mass for every short period in which the mass experiences an infinitesimal deformation. Therefore, a mechanical or kinematic assumption is prerequisite to investigate paleostresses in significantly tilted bodies.

In this paper we introduce a numerical technique to infer paleostresses from mesoscale faults in tilted rock masses. Paleomagnetists cope with such tectonic rotation using a 'bedding tilt test' or a 'fold test' (Graham, 1949; Butler, 1992) to recover initial paleomagnetic vectors. Their technique and the 'stress difference' that was recently

* Corresponding author. Tel.: +81-75-753-4166; fax: +81-75-753-4189
E-mail address: yamaji@kueps.kyoto-u.ac.jp (A. Yamaji).

0191-8141/$ - see front matter © 2004 Elsevier Ltd. All rights reserved.
doi:10.1016/j.jsg.2004.08.006

defined by Orife and Lisle (2003) inspired us to devise our testing method for paleostress analysis without a prerequisite mechanical condition, but with a kinematic one. In what follows, our testing method is explained firstly in detail, and then it is applied to artificial and natural data sets. The natural data were collected in a Lower Pleistocene sedimentary sequence in central Japan, which was folded in mid-Late Pleistocene time.

Software for the multiple inverse method (Yamaji, 2000), which was used in the testing procedure, is available from the first author.

2. Testing method

Our technique is based on the fact that syn-fold faulting results in heterogeneous fault-slip data that we observe today, and that the multiple inverse method (Yamaji, 2000) can separate reduced stress tensors from the data. Paleomagnetists obtain pre-fold magnetization if untilting of strata bundles paleomagnetic vectors to point at the same direction. If the vectors are rotated to point at a direction at the middle of back tilting, they consider syn-fold magnetization to be probable. Directional variance of the vectors is estimated by the parameter, α_{95} (Butler, 1992).

The stresses determined using the multiple inverse method are indicated by clusters in stress space. Therefore, given a measure of clustering, an untilting technique similar to that employed in paleomagnetism works to constrain paleostresses and timing of faulting relative to tilting.

For this purpose, Orife and Lisle's (2003) stress difference is useful. Assume that there are a number, N, normalized stress tensors from $\sigma^{(1)}$ through $\sigma^{(N)}$. A normalized stress tensor is deviatoric and has an octahedral shear stress of unity. The average of the tensors is given by the component-wise average:

$$\bar{\sigma} = \frac{1}{N}\left[\sigma^{(1)} + \ldots + \sigma^{(N)}\right].$$

Using the symbol, $\Delta^{(i)} = \bar{\sigma} - \sigma^{(i)}$, the stress difference between $\sigma^{(i)}$ and $\bar{\sigma}$ is written as:

$$D^{(i)} = \frac{1}{3}\left\{\left[\Delta_{11}^{(i)} - \Delta_{22}^{(i)}\right]^2 + \left[\Delta_{22}^{(i)} - \Delta_{33}^{(i)}\right]^2 + \left[\Delta_{33}^{(i)} - \Delta_{11}^{(i)}\right]^2 + 6\left[\Delta_{12}^{(i)}\right]^2 + 6\left[\Delta_{23}^{(i)}\right]^2 + 6\left[\Delta_{31}^{(i)}\right]^2\right\}^{1/2}.$$

Finally, the mean stress difference for the stresses is defined as:

$$\bar{D} = \frac{1}{N}\left[D^{(1)} + \ldots + D^{(N)}\right],$$

whose value ranges from zero to two. If all the normalized stress tensors are the same, then $\bar{D} = 0$, and the reverse is also true. $\bar{D}$ is a measure of dispersion for the given normalized stresses.

The average orientations of principal axes of the stresses are obtained as the eigenvectors of the average tensor $\bar{\sigma}$. Substituting the eigenvalues of $\bar{\sigma}$ into the equation:

$$\Phi = \frac{\sigma_2 - \sigma_3}{\sigma_1 - \sigma_3},$$

we obtain the average stress ratio $\bar{\Phi}$ for the stresses. Here, we use the sign convention that compression is positive.

For our fold test, $\bar{D}$ works just as α_{95} does in paleomagnetism. It is assumed that paleostresses responsible for faulting were spatially uniform throughout the folded beds. We use the term 'uniform' in the Euler description, just like the magnetic field is assumed to be uniform in paleomagnetic fold tests. Given a set of faults that were activated before folding or at some time during folding and were observed at different parts of a fold, progressive back tilting of fault-slip data results in a variation of $\bar{D}$. This parameter should reach the minimum when the strata from which the data were obtained are rotated backward to the situation in which the faults were created.

As mentioned in the previous section, a kinematic assumption is needed to reconcile a Cauchy stress with finite rotations. We assume that every portion of a fold kept pace with each other in tilting. That is, if the present and past dips of stratum in a portion are d_T and d, respectively, the ratio d/d_T is supposed to be spatially uniform within an area in question. The parameter $(1-d/d_T)\%$ is referred to as the amount of tilt correction in the following discussions.

3. Application to artificial data

The fold test for paleostress analysis was applied firstly to two sets of artificial fault-slip data to make an assessment of the testing method. Those data were created with the Wallace–Bott hypothesis. It was assumed that faults were observed in folded strata with an interlimb angle of 90° and a N–S-trending horizontal hinge line. The axis of rotation for back tilting was parallel to the hinge line. Fault-slip data were rotated using the software 'KUT' by Tomita and Yamaji (2003).

The two data sets had different scenarios, simple and intricate, for the history of folding and faulting. Our fold test was judged acceptable if assumed stresses and timing of faulting relative to tilting were recovered when $\bar{D}$ achieved minimum values. Natural faults are measured with errors. However, we did not include errors when creating the artificial data to exclude superfluous complexity for interpretation.

3.1. Scenario 1: syn-fold faulting

The first scenario assumed that faults were activated by horizontal compression with E–W σ_1- and vertical σ_3-axes and $\Phi = 0.6$, when the dip of limbs of a fold were 50% of

present value. That is, faulting occurred just at the middle of folding. In each of the limbs dipping at 45° in the opposite directions, 30 faults were supposed to be observed. Since the ages of faults are considered to be unknown, the faults were back-tilted beyond 50%. Fig. 1a–c shows tangent–lineation diagrams for the data sets with 0, 50 and 100% tilt correction, respectively. Paired stereograms illustrate principal axes and Φ of the stresses determined by the multiple inverse method applied to each of the sets shown by the diagrams. The data with 0% correction is identical to those we would obtain in the fold.

Blue and red arrows in the diagram show the data from the east- and west-dipping limbs, respectively. Note that fault-slip data in either of the limbs were subjected to rigid-body rotation by back tilting, because they were assumed to be generated just at the time the bedding dips were 50% of the final ones. The data indicated either by the blue or red arrows were homogeneous. When processed by the multiple inversion method, the homogeneous data sets yield the dense clusters 'A' and 'B' in Fig. 1. They consist of green to yellow squares. The colors indicate stress ratios between 0.5 and 0.7, consistent with the assumed ratio at 0.6. The two clusters were rotated with the progressive tilt correction, during which they coalesced to form the clusters 'A+B' at 50% correction (Fig. 1). They represent the correct stress that was assumed to affect the faults. Centers of the clusters are rotated by several degrees from the assumed principal stress axes, because the inverse method uses a computational grid with angular intervals of ~8° (Yamaji, 2000) and the assumed axes were not parallel to the orientations represented by the grid points. The method regards accuracy as more important than precision (Yamaji, 2003), and can

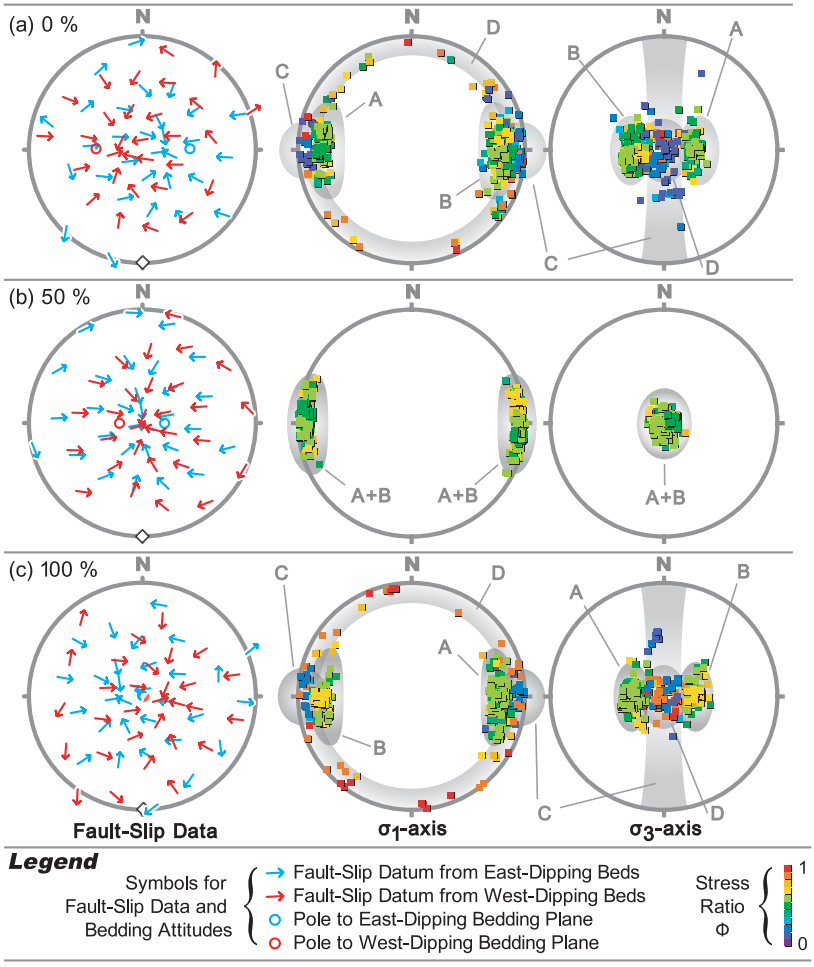

Fig. 1. Stereograms illustrating artificial fault-slip data (left column) and the results of the multiple inverse method applied to the data. To generate the artificial data it was assumed that faults were created when the beds on both limbs of a fold were inclined at 50% of the present bedding dips under the triaxial stress ($\Phi = 0.6$) with vertical σ_1- and E–W-trending σ_3-axes. Open circles in the lower-hemisphere stereonets in the left column indicate the attitudes of strata in the limbs. Their present dips are 45° and are illustrated in the upper left stereonet. The fault-slip data are shown in the same column as tangent–lineation diagrams (Twiss and Moores, 1992), on which diamonds indicate orientations of the fold hinge. It was also assumed that the relative timing of faulting was not known, therefore, the fault-slip data were back-tilted over 50% and up to 100%. The lower left stereonet illustrates the hypothetical attitudes of faults with 100% tilt correction. The middle and right columns show the results of the multiple inverse method applied to the data. Significant solutions are indicated by clusters of squares with the same color, which indicate a stress ratio. The multiple inverse method was applied with the combination number $k = 5$ and enhance factor $e = 12$. See Yamaji (2000) for the details of the parameters, k and e. These values are used throughout this paper.

separate stresses from heterogeneous data, but the solutions are smeared.

Apart from the two clusters 'A' and 'B', there are less dense clusters and girdles labeled 'C' and 'D' for tilt corrections at 0 and 100% (Fig. 1a and c). The cluster 'C' consists of blue squares, indicating nearly axial compression in E–W orientation. This is indicated by the N–S-trending girdle of blue squares in the stereonets. The cluster 'D' consists of orange to red squares. The colors indicate a nearly axial extension. Here, we follow Twiss and Moores (1992, p. 155) to refer 'axial extension' to the state of stress $\sigma_3 < \sigma_2 = \sigma_1$. The σ_3-axis is vertical, so the σ_1 orientations are indicated by a horizontal girdle.

The nearly axial stresses are false images. Their emergence was due to the faults whose slip directions are subparallel by chance to the theoretical slip directions predicted by the Wallace–Bott hypothesis with either of the stresses. As the N–S-trending axis of rotation for untilting was parallel to the σ_2-axis of the assumed stress, a part of the arrows in the tangent–lineation diagrams makes a divergent pattern from E–W orientation and a convergent pattern to the vertical. These patterns were responsible for the emergence of the axial stresses. In addition, the artificial fault planes were generated with random orientations, so that there were always some fault-slip data that were compatible with the axial stresses regardless of the amount of tilt correction. The false stresses inevitably affected the mean stress difference for the data.

Fig. 2 shows the variation of $\bar{D}$ with progressive back tilting. $\bar{D}$ became the minimum at 50% correction, consistent with the hypothesized relative timing of faulting with respect to progressive folding. At that time, $\bar{\Phi}$ was 0.58, approximately equal to the assumed $\Phi = 0.6$, and the average stress axes were nearly parallel to the assumed principal directions. Consequently, our testing method succeeded in recovering the paleostresses and in determining the timing of faulting relative to folding for this scenario.

3.2. Scenario 2: tectonic inversion

The second scenario assumes tectonic inversion: a sedimentary pile was subject initially to NE–SW horizontal extension and later to horizontal compression in the same orientation. A total of 56 faults were supposed to be observed in an anticline or a syncline. Under the first state of stress, 28 faults were supposed to be activated in horizontal beds. The later compression caused faulting of the other 28 faults when the beds were inclined at 50% of the final dips. Fig. 3a and b illustrates axes of the stresses. The 56 faults were divided into quarters, each of which was assumed to be observed at an outcrop. Two outcrops were placed on one side of a fold axis, and the remaining two were on the other side. The bedding dips at the outcrops were at 30 and 45° (Fig. 3c).

The data were back-tilted and processed using the multiple inverse method. The results are shown in Fig. 4. Clusters appeared with stress ratios near the assumed values and with orientations approximately parallel to the assumed principal axes (Fig. 3a and b). The cluster 'E' in Fig. 4

Fig. 2. Variation of mean stress difference, $\bar{D}$, by back tilting for the artificial fault-slip data shown in Fig. 1. $\bar{D}$ achieves a minimum at 50% tilt correction, because the faults were assumed to be formed when dip of the strata was 50% that of the present one.

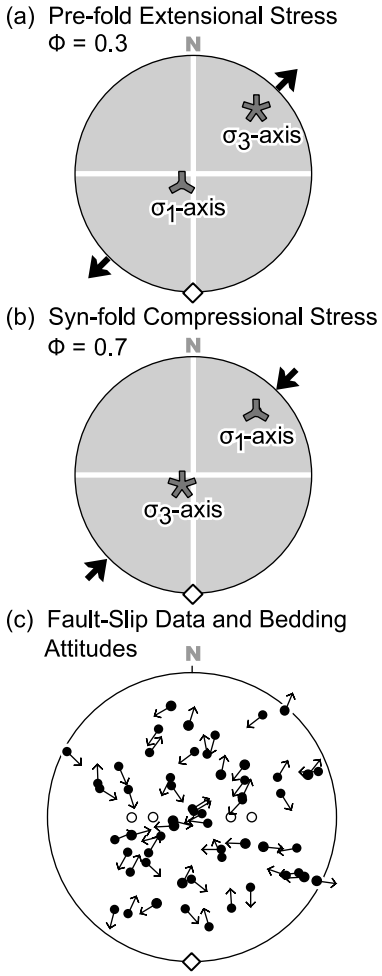

Fig. 3. Hypothetical tectonic inversion to assess the bedding tilt test for paleostress analysis in a fold structure with an interlimb angle at 90°. (a) Initial extensional stress. (b) Later syn-fold compressional stress. Red symbols indicate principal stress axes. The horizontal fold hinge was assumed to be N–S. (c) Tangent-lineation diagram showing the fault-slip data assumed to be obtained at four outcrops. Open circles designate the bedding poles at the outcrops. Diamonds indicate the orientation of fold hinge, which is used to rotate fault-slip data for back tilting.

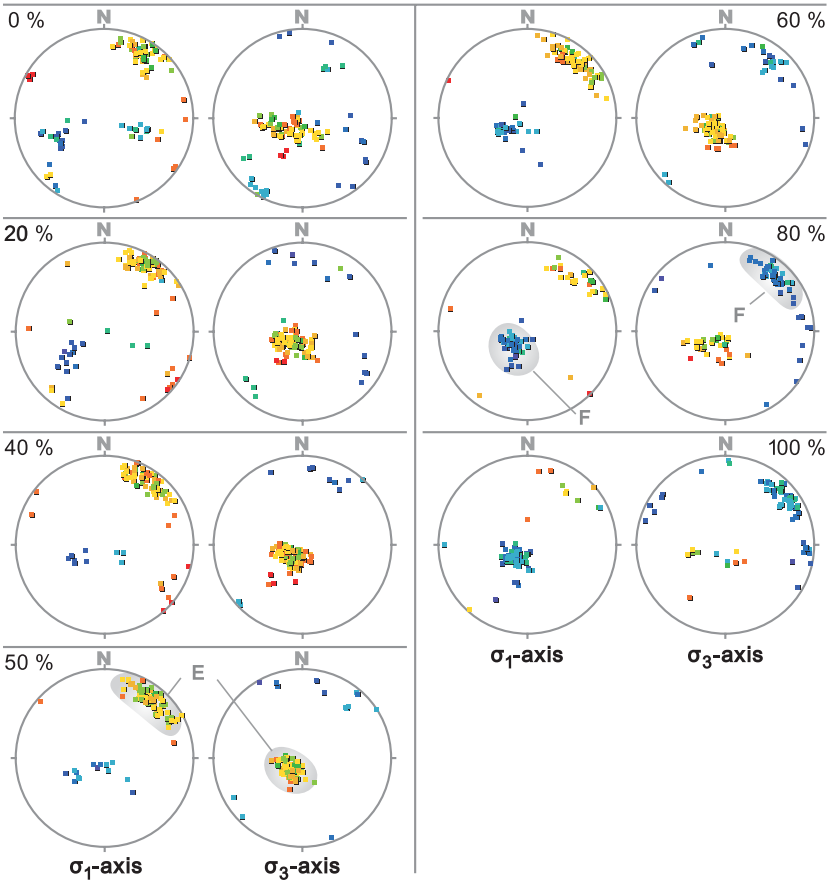

Fig. 4. Variation of stresses determined by the multiple inverse method applied to the back tilted fault-slip data in Fig. 3c. Clusters of squares on lower-hemisphere equal-area net to show the stresses. See Fig. 1 for the color codes for stress ratios. Clusters of green to yellow squares designate the syn-fold stress (Fig. 3b), and those of blue squares indicate the pre-fold stress (Fig. 3a). The hues correspond to moderately high (0.5–0.8) and low (0.1–0.4) stress ratios. The former and latter clusters in each panel are referred to as clusters 'A' and 'B', respectively.

consists of green to yellow squares, corresponding to the syn-fold compressional stress. The cluster 'F' in the same figure is composed of blue squares, corresponding to the pre-fold extensional stress.

Since we obtained clusters that were distinct in their orientations and stress ratios, it was possible to calculate mean stress difference for each of the clusters by sorting stresses in or out of the range of $0 \leq \Phi < 0.5$. Fig. 5 illustrates $\bar{D}$ versus the amount of tilt correction. The graph

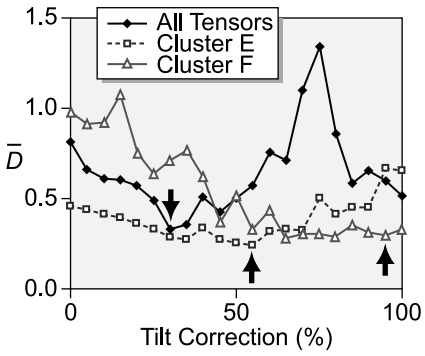

Fig. 5. Variation of mean stress difference $\bar{D}$ for the clusters in Fig. 4. Arrows point at the minimum of each line graph.

for the cluster 'E' has a roughly concave-upward shape with the minimum at 55% correction, $\bar{D}$ for the cluster 'F' largely decreases with progressive back-tilting, and achieved the minimum at 95% tilt correction. These minimal points are approximately concordant with the assumed timing of faulting relative to tilting, indicating the test method to be acceptable. The mean stress difference for the all stress tensors including those in the clusters is also shown in Fig. 5, and its graph has two minima at ~30 and 100% corrections. The gross pattern of the graph is approximately what we expect with the minimum points not far off from the amount of tilting when the faults were activated. Therefore, the back-tilting technique with the measure of $\bar{D}$ determined acceptable results for this scenario.

4. Application to natural data

4.1. Geological setting

We collected a natural data set from the Uonuma Formation, Niigata oil-and-gas field, central Japan (Fig. 6). The sedimentary basin was formed by Early Miocene

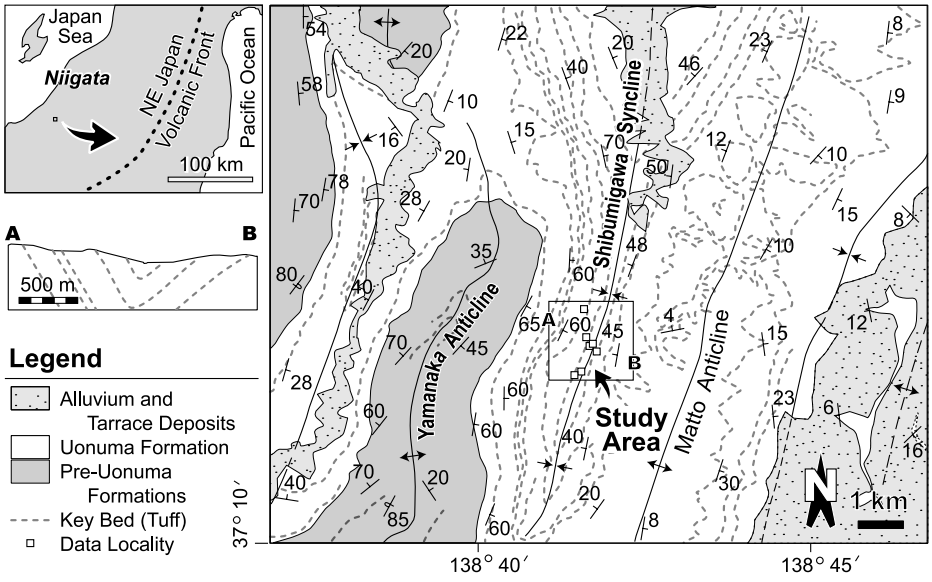

Fig. 6. Geologic map around the Shibumigawa syncline, Niigata oil field after Kobayashi et al. (1989) and Yanagisawa et al. (1986). The quadrilateral on the Shibumigawa syncline indicates the study area in which mesoscale faults were observed at seven localities around the axis of the syncline. Cross-section A–B across the study area is shown without vertical exaggeration.

rifting that resulted in the formation of the Japan Sea back-arc basin (Yamaji, 1990), and has been subject to basin inversion since the Late Miocene. The post-rift sedimentary pile is thicker than 3 km under the study area (Kobayashi et al., 1989). The sedimentary cover is folded, but map-scale faults are rare in the Niigata region. The cover is thinner in the offshore area, and faults and folds show an inverted rift system (Okamura, 2002).

The Uonuma Formation is ca. 0.7–2.2 Ma (Kurokawa, 1999), and represents a regression phase in the basin. The strata consist mainly of interbedded sandstones and siltstones with gravel and lignite layers. The stratigraphic horizon, from which we obtained the data, was composed of alluvial sediments (Kazaoka, 1988) deposited at ~1.2 Ma. This age is estimated by paleomagnetic stratigraphy (Nitobe and Niitsuma, 1971; Manabe and Kobayashi, 1988) and tephrochronology (Kurokawa, 1999; Satoguchi et al., 1999). The formation is 1.2–2.5 km thick.

We collected fault-slip data from the Shibumigawa syncline, which is ~25 km long with a NNE–SSE trend (Fig. 6). The northern part of the syncline forms a synformal depression with the hinge line plunging northward typically at ~16° to the north of the study area. A highly plunging hinge line makes bedding tilt correction uncertain, because the rotation for untilting is not unique. That is, folding and plunging may have occurred one after the other or simultaneously. We collected fault-slip data from the southern part of the syncline, where the fold is a kink fold with a subhorizontal hinge line and an interlimb angle at ~90°. The western and eastern limbs dip at about 60 and 30°, respectively (Fig. 6). The fold has an asymmetric structure: the western limb in which the dip has a little variation is 1.8 km long, whereas the eastern limbs is 0.8 km long. Our mesoscale faults were observed in the two limbs within 300 m from the fold axis and in the hinge zone, where folded surfaces have a radius of curvature of ~20 m.

Many tuff beds have been identified as key beds in the Niigata oil-and-gas field. Based on detailed mapping of the key beds and of unconformable surfaces, Kishi and Miyawaki (1996) showed that anticlines on both sides of the Shibumigawa syncline grew in the same tectonic phase, a few hundreds of thousands of years ago. Abundant normal and reverse faults in the northern and southern parts of the syncline, respectively, have been reported by Uemura and Shimohata (1972). The hinge line is gently inclined northward, so that they envisaged a neutral surface between the domains.

We chose the study area for three reasons. Firstly, there are many mesoscale faults. Secondly, old sediments may have experienced polyphase tectonics that makes interpretation difficult, but the strata themselves and their folding are young. Thirdly, the plunge of the hinge line is only 2° (Fig. 7).

4.2. Data

Twenty-four fault-slip data were collected from seven localities along the meandering Shibumigawa River. The original in-situ data are referred to as the data set with 0% tilt correction. The data are shown in Fig. 8. The observed mesoscale faults have displacements of less than 1 m. They have no or little fault gouge.

Oblique normal and strike-slip faults are dominant in the area. They trend oblique or almost perpendicular to the fold axis. This indicates that the tectonic transport parallel to the

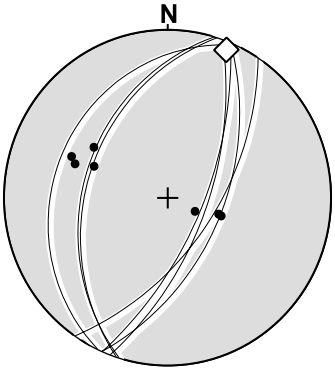

Fig. 7. Lower-hemisphere equal-angle projection in the lower right of this figure shows bedding attitudes at the localities. Great circles and small closed circles indicate the bedding and poles to them, respectively. The diamond on the stereonet shows orientation of the hinge line. Orientation of the line was determined as a principal moment of inertia of bedding poles using Johannes Duyster's software, StereoNett.

axis was not negligible. There are oblique-reverse and oblique-normal faults with dextral and sinistral sense of shear. Therefore, the data are heterogeneous. However, we had few clues to infer their relative ages.

The poles to the bedding at the localities are scattered about 90° of arc (Fig. 7). The fault-slip data were progressively rotated about the strike of bedding at each locality by 0–100% of the dip of bedding with intervals of 5% to create 21 data sets, among which seven sets are shown in Fig. 8. Back tilting makes the slip vector of the majority of the faults approach horizontal: strike-slip faults become dominant. A few oblique-normal faults remain with the pitch of their slip vectors greater than 45°. The strike-slip faults can be divided into two groups: E–W-trending dextral and NW–SE-trending sinistral faults.

4.3. Results

Results of the testing method applied to the Shibumigawa data are shown in Fig. 8. Progressive back tilting of the data from 0 to 100% affected the gross pattern of the resultant clusters to a limited extent. Namely, blue squares for σ_1- and σ_3-axes always made clusters in WNW–ESE and NNE–SSW orientations, respectively. The clusters stand for a stress regime close to strike-slip faulting of $\Phi = 0.1$–0.2. This stress ratio represents nearly axial compression; which is reflected by the appearance of denser clusters for σ_1- than for σ_3-axis. The latter axis was less accurately determined than the former. The clustering pattern was almost stationary during the back tilting for this specific data set, because most of the faults intersected the fold hinge line with high angles. Consequently, the tilt corrections insignificantly rotated the attitude of the faults, but the rake of slip vectors were rotated by a few degrees.

The densities of the clusters were significantly affected by the tilt correction. Solid lines in Fig. 9a show the variation of $\bar{D}$ versus the amount of tilt correction for all the

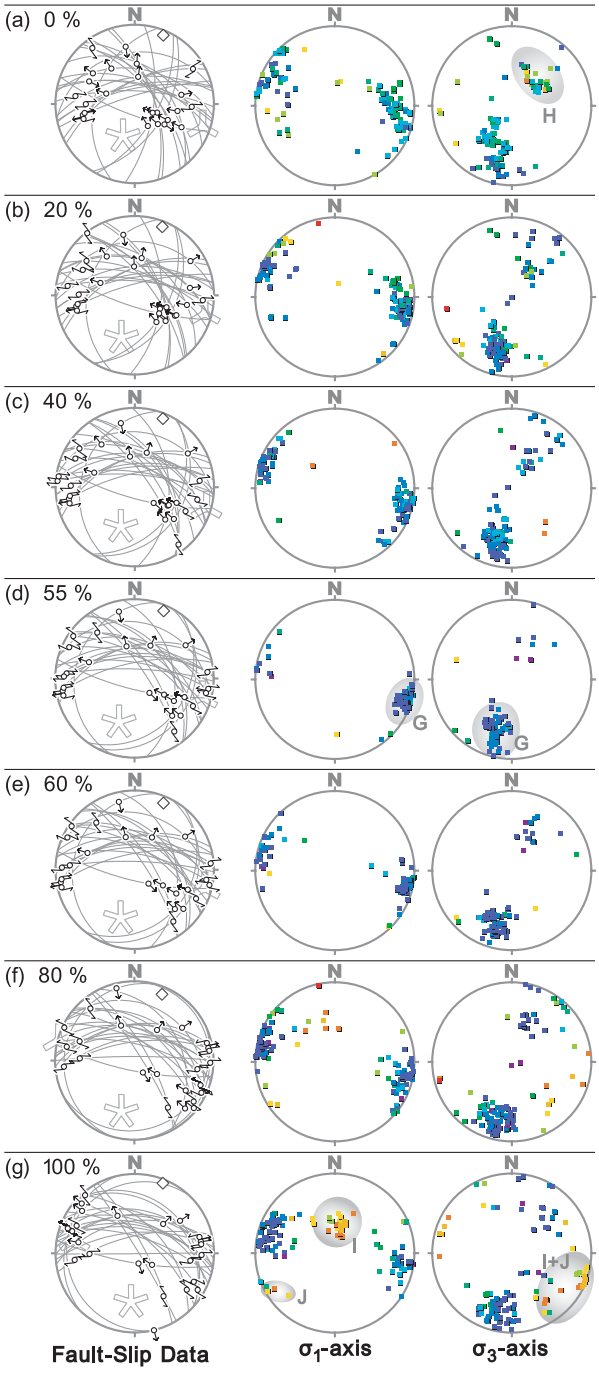

Fig. 8. Stresses determined by the multiple inverse method from the progressively back tilted fault-slip data (tangent–lineation diagrams in the left column). The data with 0% tilt correction were obtained around the axis of the Shibumigawa syncline. Floral patterns in the diagrams indicate the principal orientations of the average of the stresses shown in paired stereograms to the right of each diagram. The diamond designates hinge line of the fold, which is the axis of rotation for progressive tilt correction of the data. Note that the cluster of blue squares becomes the densest at 55% correction.

24 faults. The graph shows a concave-upward pattern with the minimum at 55% correction, suggesting that most of the faults were activated in the middle of the folding phase. The cluster labeled 'G' in Fig. 8 became the densest and the most

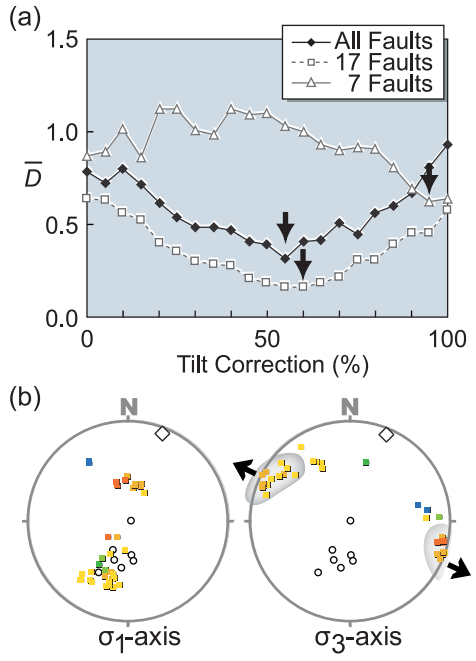

Fig. 9. (a) Variation of mean stress difference $\bar{D}$ by progressive tilt correction of the three data sets. The first one is composed of the entire 24 fault-slip data obtained in the Shibumigawa syncline; the second one came from the 17 faults that were concordant with the dense blue cluster in Fig. 7; the third one consists of the remaining seven of the 24 fault-slip data. Arrows point at the minima. (b) Paired stereograms showing the optimal stress for the seven faults at 95% tilt correction. Open circles designate the poles to the fault planes. Diamonds indicate orientation of the fold hinge line.

compact at 55% correction to represent the strike-slip faulting regime.

However, the fault-slip data at 55% tilt correction were still heterogeneous. There was one or more paleostresses other than the strike-slip faulting regime. Compatibility of the stress designated by the cluster 'G' at 55% correction to each of the faults was evaluated by the angular misfit between observed slip direction and the direction predicted from the stress. The stress was concordant for 17 faults with the misfit angles less than 30°, whereas the remaining seven faults had angles between 80 and 145°. The seven outliers were responsible for the emergence of the two other clusters in Fig. 8. One is the cluster of blue to green squares, and is labeled 'H', which was broken up by back tilting from 0 to 50%. The other one is the cluster of yellow to orange squares labeled 'I' and 'J'. The stresses represented by the last two clusters share the same σ_3 orientation, so that the clusters are labeled as 'I+J'. These clusters became evident by progressive back tilting up to 100%.

Choosing the outliers to apply the testing method shows the minimum $\bar{D}$ at 95% correction (Fig. 9a), for which result of the multiple inversion method is shown in Fig. 9b. Clusters 'I' and 'J' in Fig. 8 were enhanced in their density by extraction of the outliers. Exclusion of the seven faults was not significant for the emergence of dense cluster 'G'. Their minimum $\bar{D}$ was shifted only 5% from the minimum point of the entire faults (Fig. 9a).

Stereograms in Fig. 9b show that the stresses compatible with the outliers had a WNW–ESE extension with moderately high stress ratio. This is nearly perpendicular to the fold axis. The σ_1 orientation was less accurately determined than the σ_3 orientation because of the small number of faults and their heterogeneity. The outliers suggest that the extensional stress affected faulting in the embryonic stage of folding. The extensional stress perpendicular to the fold axis was followed by the strike-slip faulting regime with fold-perpendicular shortening in the middle of the folding.

5. Discussion

Paleostress analysis in significantly tilted rock mass has a theoretical difficulty as we mentioned in Section 1 The difficulty comes from the discrepancy between the Euler and Lagrange descriptions of stresses for finite deformations. We need some assumption to get paleostresses, unless we know the complete deformation history of the mass including timing of the movement of each fault.

For this reason, mechanical considerations are often used. Before stress inversion became popular, Mohr's hypothesis of failure (Jaeger and Cook, 1979) was used, because it allows one-to-one correspondence of a fault with the principal orientations of the responsible stress with an assumed angle of shear. However, modern stress inversion is based not on Mohr's but on the Wallace–Bott hypothesis (Angelier, 1994). Several authors assume Anderson-type faulting (Uemura and Shimohata, 1972), neglecting oblique faults that are commonly observed (Bott, 1959). Other researchers rely on the fact that a stress axis is oriented nearly vertical at shallow levels of the crust (e.g. Martin and Bergerat, 1996; Fabbri, 2000; Vandycke and Bergerat, 2001). However, in-situ stress measurements have revealed that this is not always true (Engelder, 1992; Amadei and Stephansson, 1997). The assumption is improbable a priori, specifically at shallow levels of active zones like the Niigata district where we collected fault-slip data in this study. The reason is that tectonic activity amplifies undulations of a topographic surface and of subsurface density interfaces. Horizontal density variations are the results of the undulations, and the variations rotate stress axes (Sonder, 1990).

We have proposed an alternative method to infer paleostresses in highly tilted blocks. Instead of these mechanical considerations, we set up paleostress analysis with a kinematic hypothesis. Namely, it was considered that every part of a fold kept pace with each other in tilting and has an identical normalized stress tensor. These assumptions reduce the utility of the testing method. However, satisfactory results were obtained for the artificial data sets that suited the hypothesis. We believe that the method is worth applying to faults whose classification is difficult. It

should be noted also that the method is useful for faults not only in folds but also in blocks tilted by extensional tectonics, provided that they have a similar strike of bedding.

Regarding the faults in the Shibumigawa syncline, the following facts support applicability of our method. Firstly, limbs of the syncline are thought to be tilted in the same tectonic phase (Kishi and Miyawaki, 1996). Secondly, the hinge line is approximately horizontal, so that the rotational operation for back tilting had little ambiguity in choosing the axis of rotation.

It was inferred that a strike-slip faulting regime of stress activated most of the observed faults in the syncline. This seems discordant with folding, because folding causes horizontal shortening and vertical extension of a sedimentary package. This strain fits a reverse-faulting regime of stress. We suggest that flexural folding was the primary mechanism responsible for the fold-perpendicular extensional stress in the embryonic folding state and for strike-slip regime in the middle of the folding phase. We may have detected a local stress rather than a regional stress that formed the fold belt. Sedimentary layers are kinked at the Shibumigawa syncline. Kink folds develop in strongly layered sequences that have a strong planar mechanical anisotropy (Twiss and Moores, 1992). The sedimentary rocks that we observed in the syncline may have been mechanically decoupled by flexural slips from the reverse-faulting stress regime under the syncline. We interpret the fold-perpendicular initial extension as that in the convex side of neutral surface; we follow the suggestion by Uemura and Shimohata (1972) who inferred syn-fold paleostresses with the assumption of Anderson-type faults. To verify the hypotheses for the relationship between folding and faulting in the syncline, we have to extend our study area.

Acknowledgements

We thank S. Vandycke and anonymous reviewers for the improvement of the manuscript and T. Blenkinsop for English editing. Discussions with T. Imamura and Y. Yamada were appreciated. This work was financially supported by JSPS (No. 14540423).

References

Amadei, B., Stephansson, O., 1997. Rock Stress and its Measurement. Chapman and Hall, London.

Angelier, J., 1994. Fault slip analysis and paleostress reconstruction, in: Hancock, P.L. (Ed.), Continental Deformation. Pergamon Press, Oxford, pp. 53–101.

Angelier, J., Colletta, B., Anderson, R.E., 1985. Neogene paleostress changes in the Basin and Range: a case study at Hoover Dam, Nevada-Arizona. Geological Society of America Bulletin 96, 347–361.

Angelier, J., Barrier, E., Hao, T.C., 1986. Plate collision and paleostress trajectories in a fold–thrust belt: the foothills of Taiwan. Tectonophysics 125, 161–178.

Bott, M.H.P., 1959. The mechanics of oblique slip faulting. Geological Magazine 96, 109–117.

Butler, R.F., 1992. Paleomagnetism: Magnetic Domains to Geologic Terrains. Blackwell Scientific Publisher, Boston.

Choi, P.Y., Kwon, S.K., Hwang, J.H., Lee, S.R., An, G.O., 2001. Paleostress analysis of the Pohang–Ulsang area, southeast Korea: tectonic sequence and timing of block rotation. Geoscience Journal 5, 1–18.

Engelder, T., 1992. Stress Regimes In The Lithosphere. Princeton University Press, Princeton.

Fabbri, O., 2000. Extensional deformation in the northern Ryukyu arc indicated by mesoscale fractures in the middle Miocene deposits of Tanegashima Island. Journal of Geological Society of Japan 106, 234–243.

Fung, Y.C., 1965. The Foundations of Solid Mechanics. Prentice-Hall, Englewood Cliffs.

Graham, J.W., 1949. The stability and significance of magnetism in sedimentary rocks. Journal of Geophysical Research 54, 131–167.

Jaeger, J.C., Cook, N.G.W., 1979. Fundamentals of Rock Mechanics, 3rd ed Chapman and Hall, London.

Kazaoka, O., 1988. Stratigraphy and sedimentary facies of the Uonuma Formation in the Higashikubiki Hills, Niigata Prefecture, central Japan. Chikyu Kagaku 42, 61–83.

Kishi, K., Miyawaki, R., 1996. Plio-Pleistocene fold development in the Kashiwazaki Plain and vicinity, Niigata Prefecture. Journal of Geography 105, 88–112.

Kobayashi, I., Tateishi, M., Kurokawa, K., Yoshimura, T., Kato, H., 1989. Geology of the Okanomachi district with geological sheet map at scale 1:50,000. Geological Survey of Japan.

Kurokawa, K., 1999. Tephrostratigraphy of the Nanatani to Uonuma Formations of 13 Ma to 1 Ma in the Niigata region, central Japan. Journal of the Japanese Association for Petroleum Technology 64, 80–93.

Manabe, K., Kobayashi, I., 1988. Magnetostratigraphy of the Plio-Pleistocene in the Niigata sedimentary basin, central Japan. Journal of Geological Society of Japan 94, 103–112.

Martin, P., Bergerat, F., 1996. Paleo-stresses inferred from macro- and micro-fractures in the Balazuc-1 borehole (GPF programme). Contribution to the tectonic evolution of the Cévennes border of the SE basin of France. Marine and Petroleum Geology 13, 671–684.

Nitobe, T., Niitsuma, N., 1971. Paleomagnetic and pollen stratigraphy of the Uonuma Group. Daiyonki Kenkyu 10, 38–39.

Okamura, Y., 2002. Deformation zone since Neogene in the eastern margin of Japan Sea, in: Satake, M., Taira, A., Ota, Y. (Eds.), Active Faults and Seismotectonics in the Eastern Margin of Japan Sea. University of Tokyo Press, Tokyo, pp. 111–121.

Orife, T., Lisle, R.J., 2003. Numerical processing of palaeostress results. Journal of Structural Geology 25, 949–957.

Pollard, D.D., Saltzer, S.D., Rubin, A.M., 1993. Stress inversion methods: are they based on faulty assumptions? Journal of Structural Geology 15, 1045–1054.

Satoguchi, Y., Nagahashi, Y., Kurokawa, K., Yoshikawa, S., 1999. Tephrostratigraphy of the Pliocene to lower Pleistocene formations in central Honshu, Japan. Chikyu Kagaku 53, 275–290.

Sonder, L.J., 1990. Effects of density contrasts on the orientation of stresses in the lithosphere; relation to principal stress directions in the Transverse Ranges, California. Tectonics 9, 761–771.

Tomita, S., Yamaji, A., 2003. KUT: software to rotate orientation data. Geoinformatics 14, 85–104.

Twiss, R.J., Moores, E.M., 1992. Structural Geology. Freeman, New York.

Twiss, R.J., Unruh, J.R., 1998. Analysis of fault slip inversions: do they constrain stress or strain rate? Journal of Geophysical Research 103, 12205–12222.

Uemura, T., Shimohata, I., 1972. Neutral surface of a fold and its bearing on folding. 24th International Geological Congress, Section 3 1972; 599–604.

Vandycke, S., Bergerat, F., 2001. Brittle tectonic structures and paleostress analysis in the Isle of Wight, Wessex basin southern UK. Journal of Structural Geology 23, 393–406.

Yamaji, A., 1990. Rapid intra-arc rifting in Miocene Northeast Japan. Tectonics 9, 365–378.

Yamaji, A., 2000. The multiple inverse method: a new technique to separate stresses from heterogeneous fault-slip data. Journal of Structural Geology 22, 441–452.

Yamaji, A., 2003. Are the solutions of stress inversion correct? Visualization of their reliability and to separate stresses from heterogeneous fault-slip data. Journal of Structural Geology 24, 241–252.

Yanagisawa, Y., Kobayashi, I., Takeuchi, K., Tateishi, M., Chihara, K., Kato, H., 1986. Geology of the Ojiya district with geological sheet map at scale 1:50,000. Geological Survey of Japan.